# Atomization Process of an Annular Liquid Sheet assisted by an Inner Gas Jet

N. Leboucher*, F. Roger, J. L. Carreau and A. Claverie
Laboratoire de Combustion et de Détonique, CNRS UPR 9028
University of Poitiers
ENSMA, 1 Avenue Clément Ader, BP 40109, 86961 Chasseneuil Futuroscope, France

**Abstract**

In order to design new injectors in cryogenic propulsion, the atomization process of an annular liquid sheet assisted by a swirling inner gas jet with different ambient pressures is studied. The liquid used is water, the gas is air and three experimental techniques are performed. First, films at 12 500 and 14 000 frames per second show the behavior of the liquid sheet. Second, laser tomography is used to determine the break-up length. At last, axial and radial velocities as well as diameter are determined for droplets measuring from 5 to 230 µm by Phase Doppler interferometry (PDI). Basically, two break-up mechanisms are identified with high speed visualizations, namely bubble formation and “Christmas tree”. The frequency of bubble formation and “Christmas tree” is related to gas and liquid velocities, gas and liquid densities and swirl intensity. In “Christmas tree mode”, the tomography shows that the break-up length decreases with gas to liquid momentum flux ratio (J), swirl intensity, and without significant effect of ambient pressure. The droplets have high radial velocities and their mean axial velocities grow with J and decline with ambient pressure. Last, the gas swirl enlarges the previous radial profile, promotes a better primary atomization, and allows better homogenization of the droplet axial velocities. The Sauter Mean Diameter (SMD) of the liquid droplets increases slightly with radial and axial distances, showing that primary and secondary atomizations are very fast.

## Introduction

The understanding and control mechanisms of atomization are very important for liquid propellant rocket engines ($H_2/L_{OX}$), to ensure the stabilization of combustion process. Most of these engines used coaxial high speed gas jet to promote the pulverization of the liquid jet and, consequently, the chemical reaction efficiency. Therefore, numerous studies are done in this field, most of them by using water and air in order to represent liquid oxygen and gaseous hydrogen mixing. The fundamental difference is the surface stresses because liquid oxygen is supercritical in rocket engines. To enhance atomization, new designs are developed, one of them considering the pulverization of an annular liquid sheet by an inner gas jet. In this configuration, Choi and Lee [1] identified three disintegration modes namely, Rayleigh, bubble break-up and pure-pulsating. Moreover, in Rayleigh mode, cell structures are visible on the surface of the bubbles. With two coflowing gas streams, Lavergne et al. [2] distinguished three regimes of break-up: (i) bubble formation (Rayleigh), (ii) wind-induced and, (iii) atomization. They also investigated, with a microphone, the instability frequency of the sheet and found that it increases with gas velocity but only slightly with outer gas swirl. Adzic et al. [3] described the following regimes, Kelvin-Helmholtz, cellular and atomization. The first is divided into three submodes: the Rayleigh regime occurs at low inner gas velocity and without significant outer gas velocity; the second submode is shaped like a “Christmas tree” at the injector exit; then, the last submode is characterized by Kelvin-Helmholtz instabilities visible on the sheet surface. Eventually, the disintegration regime due to the striking appearance of cells is termed cellular regime and when the sheet in atomized at the injector exit, the atomization regime is reached. Kawano et al. [4] studied the wave propagation on the gas liquid interface and noticed that the deformation amplitude of the sheet rises downstream until its rupture. Moreover, they observed a coincidence between the oscillation frequency and the classical gaseous Weber number for a liquid velocity higher than 3 m/s. Like Lavergne et al. [2], the frequency increases with the gas velocity, but it rises until a liquid velocity of 3 m/s and then declines slightly. More recently, the oscillations of a plane liquid sheet assisted by two coflowing gas streams have been investigated. Lozano et al. [5] studied the resulting flow close to the injector exit and noticed that the oscillation frequency is proportional to the air velocity for a fixed liquid velocity. Moreover, for a fixed air velocity and varying water velocity, the SMD presents a minimum roughly coincident with the maximum frequency. In agreement with Ref. [5], Carvalho et al. [6] observed a rise of the frequency with air velocity but a complex liquid velocity effect. However, they suggested a relation between a Strouhal number - based on the liquid velocity and sheet thickness - with *J*. Lozano et al. [7] showed that the frequency *f* depends on the sheet thickness *e* and defined a

* Corresponding author: nicolas.leboucher@lcd.ensma.fr

Strouhal number $St$ (1), $d_A$ and $U_A$ representing the velocity and thickness of the coflowing air streams and $U_{min}$ the minimum air velocity for which the sheet oscillation appears.

$$St = \left( f\sqrt{e \cdot d_A} \right) \Big/ \left( U_A - U_{min} \right) \quad (1)$$

Like Adzic et al. [1] and Lavergne et al. [2], Cao [8] observed a decreasing break-up length with air velocity but also noted its periodical variation. Li and Shen [9] analyzed the spray produced by an annular liquid sheet assisted by two coflowing air streams in the intermediate and far fields; their major conclusions are following: (i) the inner gas promotes a better atomization than the outer gas, (ii) the radial profile of the mean axial velocity is Gaussian, (iii) the SMD of the produced droplets increases from the spray centerline to the periphery. Leboucher et al. [10] investigated the flow field close to the injector exit in a similar configuration and found the following results: (i) the primary atomization becomes faster, the mean droplet axial velocity rises and the SMD decays with $J$; (ii) the mean droplet axial velocity drops whereas the SMD increases slightly with ambient pressure; (iii) a strong inner gas swirl promotes the primary atomization, enlarges the half property of the radial profile of mean droplet axial velocity and homogenizes the droplets velocities. Studying a round liquid jet assisted by an annular gas stream, Prevost et al. [11], found a faster break-up of the liquid jet and an increasing mean droplet diameter in the periphery of the spray with ambient pressure. In a similar configuration Porcheron et al. [12] have studied the gas density effect considering Helium, Nitrogen or Argon.

Few articles dealt with the mechanisms of atomization and oscillation frequency of assisted liquid sheets and the properties of the spray are investigated only under atmospheric pressure. In this article, we present the atomization processes, the break-up length, velocities and SMD of droplets obtained from an annular liquid sheet assisted by an inner swirling gas jet under different ambient pressures.

**Materials and Methods**

The experimental setup, called JETCOAP, is carefully described in [13]. A compressor supplies the injector with air and allows a range of ambient pressure varying from 0.1 to 0.9 MPa. It is divided into two main parts: one is dedicated to injector positioning and fluid inlets; the second ensures pressure control and fluid evacuation and is devoted to measurement techniques. Tomography and PDA techniques are possible thanks to four optical accesses, with one placed at 60° with respect to the horizontal dedicated to the reception of the PDA. The injector is basically made up by co-axial tubes (Figure 1) mounted on displacement tables motorized in two directions with a precision of 10 µm and a stainless steel braided extensive cylinder enables connection between the chamber and tables. The diameter of the gas jet is 2.5 mm and the 500 µm thickness liquid sheet has an outer diameter of 4 mm.

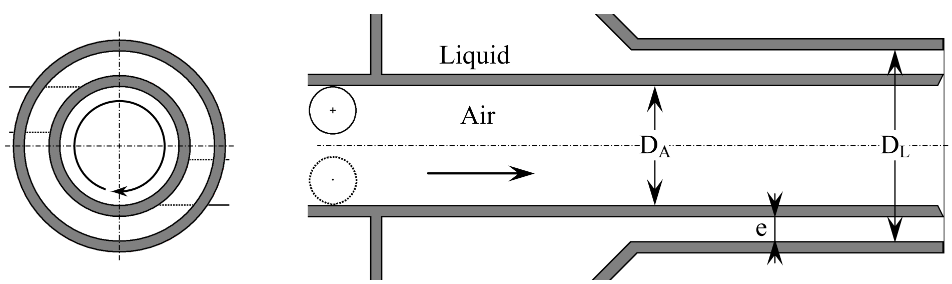


**Figure 1.** Injector characteristics

The fluids used are air and water. A water-meter and a by-pass system are used to adjust the liquid velocity at the exit to 1, 2 or 5 m/s. Two flowmeters, a thermocouple and a pressure transducer allow the determination of gas density and gas velocity at the injector exit. Two tangential inlets displaced from the injector axis allow a rotation of the gas until a maximum swirl intensity of 0.95 [14]. This intensity is defined in (2), with $R$ the tube radius, $U_B$ the bulk axial velocity, $U$ and $W$ the axial and tangential velocities respectively.

$$\Omega = \int_0^R U\,W\,r\,dr \Big/ R^2 U_B^2 \quad (2)$$

In this study, a Photron RS3000 high speed camera allows visualizations at 12 500 and 14 000 frames per second. Two methods have been performed: the first is a backlight using a 500 W halogen lamp and the second is a high speed laser tomography enabled by a 300 µm thickness laser sheet generated by a diode pumped solid state laser and centered on the flow axis. Previously, a low speed tomography (laser sheet thickness of 500 µm), also centered on the flow axis, had been carried out with a Nd-Yag laser and a CCD camera FlowMaster 3S La Vision. The PDI used is a Dantec system composed with an Argon laser, wavelength beams of 514.5 and 488 nm, coupled with a transmitter fitted with 600 mm focal length lens and a receiver (600 mm focal length also), oriented at 60° from the forward direction of the transmitter axis. This technique allows the determination of axial and radial velocities, and droplet diameter measuring from 5 to 230 µm. The number of samples is 5000 within a time limit set at 60 s and the spherical validation criterion is set to 10%. The precision of this method is better than 10%, but is 20% for the SMD.

The gas momentum flux distribution is determined with a 0.5 mm thickness Pitot tube (0.32 mm inside) placed at 0.5 mm downstream from the injector exit for a mass flow rate of 0.62 g/s (Figure 2), and integrated. The gas density, deduced from this integral and the mass flow-rate, allows us the following hypothesis: if the upstream pressure is lower than the critical value, the flow is considered as an isentropic expansion; else, the hypothesis of sonic orifice is done and the flow between the inlets and the injector exit is considered isotherm, due to the heat transfer between the liquid circuit and the inner gas. The gas velocity varies from 25 to 300 m/s, the ambient pressure from 0.1 to 0.7 MPa allowing a density between 1.2 and 9.1 kg/m$^3$. The precision for these parameters is better than 5 %.

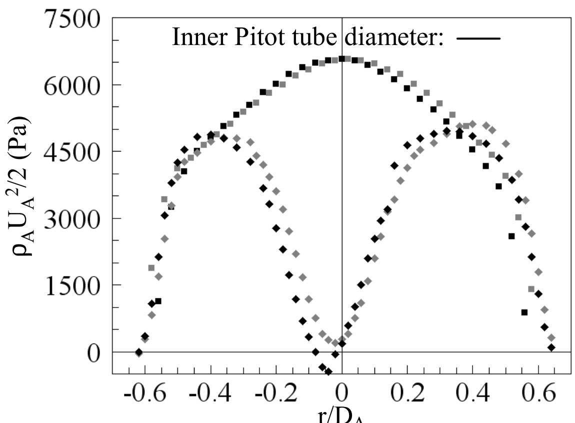


**Figure 2.** $\rho_A U_A^2/2$ profile obtained with a Pitot tube ($m_A$ = 0.62 g/s, $P_a$ = 0.1 MPa)
■ Ω = 0, vertical ◆ Ω = 0.95, vertical ■ Ω = 0, horizontal ◆ Ω = 0.95, horizontal

**Results and Discussion**

Two main break-up mechanisms are identified with fast visualization methods: bubble formation and “Christmas tree”. Two behaviors are observed for the first mode at low air velocity (25 m/s): for a low liquid velocity (1 m/s), a bubble is periodically formed at the injector exit, but because of the small inertia force of the liquid and a great difference between gas and liquid velocity, it finally bursts; for faster liquid velocity (2 and 5 m/s), a stable bubble train is formed and cellular structures can be seen on their surface (Figure 3).

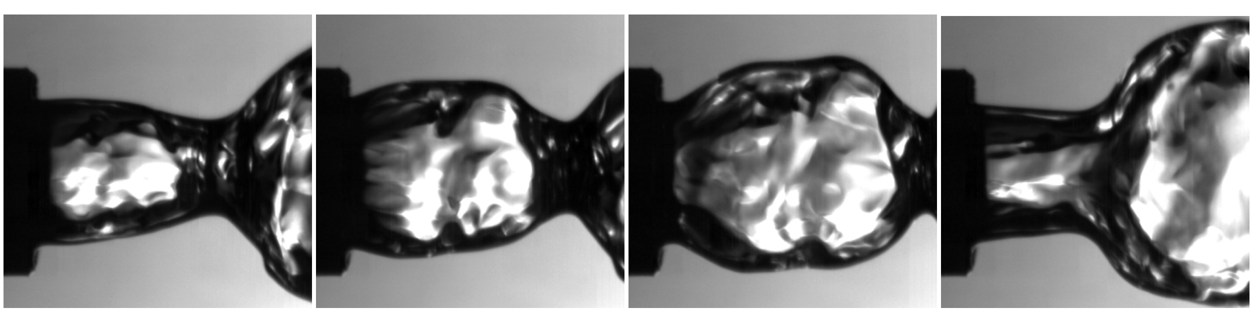

t = 0 t = 0.43 ms t = 0.93 ms t = 2.43 ms

**Figure 3.** High speed visualization sequence ($U_L$ = 2 m/s, $U_A$ = 25 m/s, Ω = 0 and $P_a$ = 0.1 MPa)

The second mode called "Christmas tree" exists for higher gas velocity (Figure 4): a bubble starts forming at the injector exit but is fed by air faster than previously, and when the pressure inside becomes too high, it bursts producing droplets with high radial velocity and the resulting flow seems shaped like a "Christmas tree".

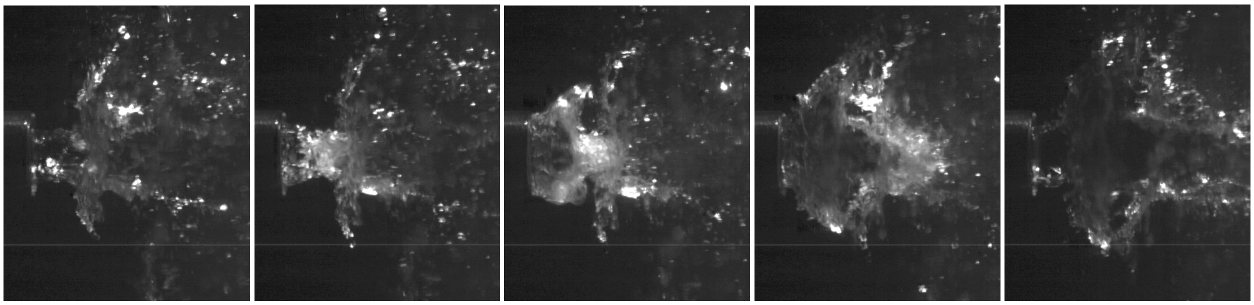

t = 0 t = 0.21 ms t = 0.43 ms t = 0.86 ms t = 1.29 ms

**Figure 4.** High speed tomography sequence ($U_L$ = 2 m/s, $U_A$ = 99 m/s, Ω = 0 and $P_a$ = 0.1 MPa)

The visualizations of the bubble formation and "Christmas tree" are characterized by a periodic variation of the luminous intensity close to the injector exit. This luminous signal is slow down and integrated by an Ultrafast Photodetector UPD optical device and recorded on a digital oscilloscope. A Fast Fourier Transform (FFT) determines the frequency *f* of the phenomenon (Figure 5) with a precision equal to 5 % approximately. At last, when the contrast is low, a counting is done to validate the measurement.

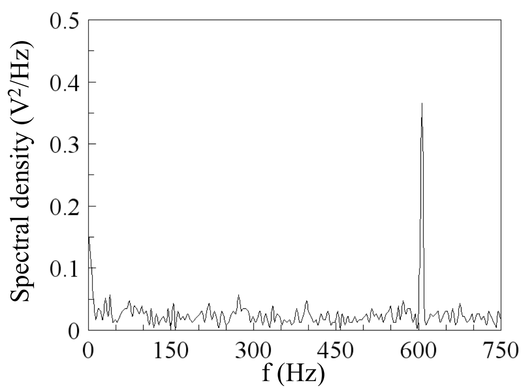


**Figure 5.** FFT example ($U_L$ = 5 m/s, $U_A$ = 25 m/s, Ω = 0 and $P_a$ = 0.1 MPa)

The frequency rises with air and liquid velocities, gas density and swirl intensity. Like Kawano et al. [4], at low gas velocity (25 m/s) and liquid velocity (1 m/s), the peak of the FFT spectrum is wider than the other conditions due to a more irregular behavior. High gas velocity (200 m/s) promotes atomization, the "Christmas tree" becomes hardly observable and the frequency is not measurable.

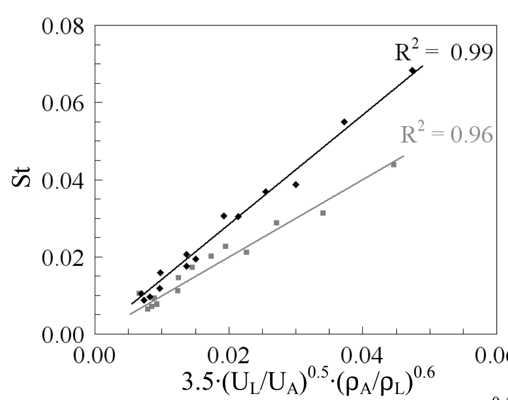


**Figure 6.** Correlation between the Strouhal number and $3.5 \cdot (U_L/U_A)^{0.5}(\rho_A/\rho_L)^{0.6}$, ■ Ω = 0 ◆ Ω = 0.95

The Strouhal number defined by Lozano [7], is related by a dimensionless analysis to the exit conditions. The results, shown (3) and Figure 6, are obtained by a multiple non linear regression by least squares method, with a correlation coefficient of 0.98, and $U_{min}$ = 10 m/s comparable with the results of Ref. [7]. The gas and liquid velocities have equal influence on the frequency.

$$St = 3.5\left(U_A/U_L\right)^{-0.5}\left(\rho_A/\rho_L\right)^{0.6}\left(1+0.42\cdot\Omega\right) \qquad (3)$$

The following results deals with the "Christmas tree" mode. In agreement with Cao [8], the periodical variation of the break up length is observed with films, and tomography shows that it can quadruple. The mean break up length is determined by the mean and root mean square of 200 images. It decreases with $J$ (= $\rho_G U_G^2/\rho_L U_L^2$) and swirl intensity and without significant effect of ambient pressure (Figure 7).

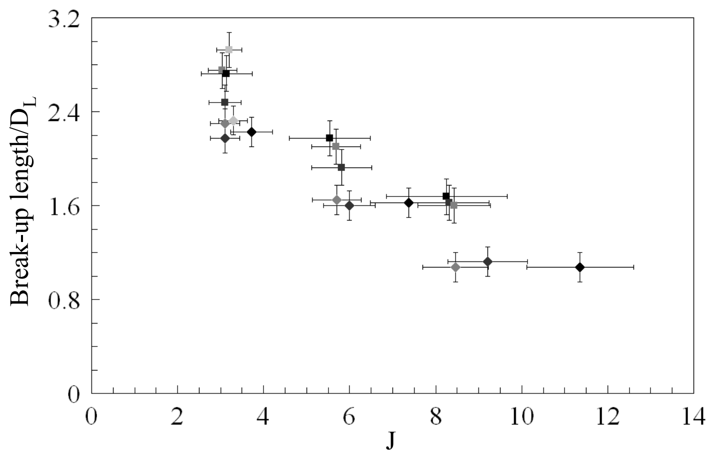


**Figure 7.** Break-up length evolution with $J$, ■ Ω=0, Pa=0.1 MPa ◆ Ω=0.95, Pa=0.1 MPa ■ Ω=0, Pa=0.3 MPa ◆ Ω=0.95, Pa=0.3 MPa ■ Ω=0, Pa=0.5 MPa ◆ Ω=0.95, Pa=0.5 MPa ■ Ω=0, Pa=0.7 MPa ◆ Ω=0.95, Pa=0.7 MPa

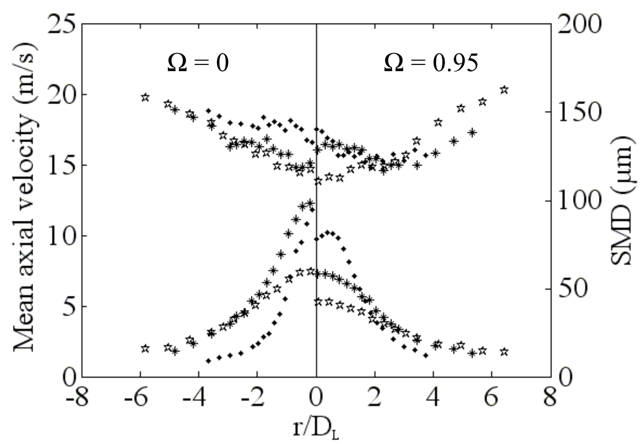


**Figure 8.** Mean axial velocity (bottom) and SMD (top) at three different locations, $J_C$ = 3 and Pa = 0.5 MPa without and with swirl, ⬩ X = 2.5 $D_L$ ✻ X = 7.5 $D_L$ ☆ X = 15 $D_L$

PDI technique is performed at ambient pressure equal to 0.3, 0.5 and 0.7 MPa, because under atmospheric pressure, droplets with high radial velocity pollute optical accesses. Radial profiles is carried out to abscissas $X$ = 2.5, 5, 7.5, 11.25, 15 and 18.75 $D_L$ from the injector exit. The mean droplet axial velocity rises with $J$ but decreases with gas swirl and ambient pressure. Gas swirl homogenizes axial velocities of droplets and raises the half property of their mean radial profile. Moreover, the maximum value is reached faster proving a better primary atomization (Figure 8). For $X$ = 2.5 $D_L$, the maximum value of the mean droplet radial velocity increases with gas swirl but becomes comparable for next abscissa. Nearly, all root mean square of droplet radial velocities decline with gas swirl effect explaining that optical was less polluted. SMD of liquid droplets increases slightly with radial and axial distances, showing that primary and secondary atomizations are very fast. Near the injector and the spray axis, the SMD and the mean velocities of droplets are affected by a huge drop of the validation rate corresponding to the liquid sheet. The comparison with Ref. [13] – considering the same droplet diameter detection (5-145 µm) – shows here a better atomization, the SMD values are lower although more liquid is injected (1.3 times higher).

**Conclusions**

In this article, two main break-up mechanisms of an annular liquid sheet assisted by an inner swirling gas jet are identified, bubble formation and "Christmas tree". The frequency of their formation increases with air and liquid velocities, gas density and swirl intensity. The mean break-up length decreases with *J*, swirl intensity and without significant effect of ambient pressure. The primary and secondary atomizations are very fast, the droplets have a high radial velocity and their mean axial velocity grows with *J* and a decreasing ambient pressure. At last, the gas swirl enlarges the previous radial profile, promotes a better primary atomization, and allows a better homogenization of the droplet velocities. Of course, it will be interesting to find out a relation between the frequency and the mean droplet diameter.

**Acknowledgements**

The authors acknowledge financial support from CNRS and the Poitou-Charentes region.

**Nomenclature**

$e$ sheet thickness
$f$ sheet oscillation frequency
$J$ gas to liquid momentum flux ratio
$St$ Strouhal number
$U$ axial velocity
$U_B$ bulk axial velocity
$W$ tangential velocity
$\Omega$ swirl intensity
$\rho$ density

Subscripts
$A$ air
$L$ liquid
a ambient

**References**

1. Choi C.J., Lee S.Y., *Seventh International Conference on Liquid Atomization and Spray Systems*, Seoul, Korea, August 1997, pp. 255-261.
2. Lavergne G., Trichet P., Hebrard P., Biscos Y., *J. Eng. Gas Turbines Power*, 115:461-466 (1993).
3. Adzic M., Carvalho I.S., Heitor M.V., *Optical diagnostics in Eng.*, 5:27-38 (2001).
4. Kawano S., Hashimoto H., Togari H., Ihara A., Suzuki T., Harada T., *Atomization and Sprays*, 7:359-374 (1997).
5. Lozano A., Barreras F., Hauke G., Dopazo C., *J. Fluid Mech.*, 437:143-173 (2001).
6. Carvalho I.S., Heitor M.V., Santos D., *Int. J. Multiphase Flow*, 28:773-789 (2002).
7. Lozano A., Barreras F.,Siegler C., Löw D., *Experiments in Fluids*, 39:127-139 (2005).
8. Cao J., *J. Automobile Eng.*, 217:735-743 (2003).
9. Li X., Shen J., *J. Propulsion Power*, 15:103-110 (1999).
10. Leboucher N., Laporte G., Carreau J. L., Roger F., *twenty-first Annual Conference on Liquid Atomization and Spray Systems*, Mugla, Turkey, Sept 2007.
11. Prevost L., Carreau J. L., Porcheron E., Roger F., *fifteenth Annual Conference on Liquid Atomization and Spray Systems*, Toulouse, France, July 1999.
12. Porcheron E., Carreau J. L., Prevost L., Le Visage D., Roger F., *Atomization and Sprays*, 12:209-227 (2002).
13. Dunand A., Carreau J. L., Roger F., *Atomization and Sprays*, 15:223-247 (2005).
14. Chang F., Dhir V.K., *Int. J. Heat Fluid Flow*, 15:5:346-356 (1994).